Journal of Biomolecular NMR, **15:** 213–225, 1999.
KLUWER/ESCOM

Solvation study of the non-specific lipid transfer protein from wheat by intermolecular NOEs with water and small organic molecules

Edvards Liepinsh[a], Patrick Sodano[b,*], Severine Tassin[b], Didier Marion[c], Françoise Vovelle[b] & Gottfried Otting[a,**]

[a]*Karolinska Institutet, Department of Molecular Biochemistry and Biophysics, S-171 77 Stockholm, Sweden;* [b]*Centre de Biophysique Moléculaire, rue Charles Sadron, F-45071 Orléans Cedex 02, France;* [c]*Laboratoire de Biochimie et Technologie des Proteines, INRA, rue de la Géraudière, F-44316 Nantes Cedex 05, France*

Received 14 June 1999; Accepted 17 September 1999

Key words: gas phase NMR, homonuclear pulse sequences, intermolecular NOE, lipid transfer protein, non-polar cavity, occupancy, protein hydration, protein–solvent interaction

Abstract

Intermolecular nuclear Overhauser effects (NOEs) were measured between the protons of various small solvent or gas molecules and the non-specific lipid transfer protein (ns-LTP) from wheat. Intermolecular NOEs were observed with the hydrophobic pocket in the interior of wheat ns-LTP, which grew in intensity in the order cyclopropane (saturated solution) < methane (140 bar) < ethane (40 bar) < acetonitrile (5% in water) < cyclohexane (saturated solution) < benzene (saturated solution). No intermolecular NOEs were observed with dioxane (5% in water). The intermolecular NOEs were negative for all of the organic molecules tested. Intermolecular NOEs between wheat ns-LTP and water were weak or could not be distinguished from exchange-relayed NOEs. As illustrated by the NOEs with cyclohexane versus dioxane, the hydrophobic pocket in wheat ns-LTP preferably binds non-polar molecules. Yet, polar molecules like acetonitrile can also be accommodated. The pressure dependence of the NOEs between methane and wheat ns-LTP indicated incomplete occupancy, even at 190 bar methane pressure. In general, NOE intensities increased with the size of the ligand molecule and its vapor pressure. NMR of the vapor phase showed excellent resolution between the signals from the gas phase and those from the liquid phase. The vapor concentration of cyclohexane was fivefold higher than that of the dioxane solution, supporting the binding of cyclohexane versus uptake of dioxane.

Introduction

Small organic solvent molecules have been shown to bind preferentially to internal, non-polar cavities in proteins (Morton et al., 1995; Feher et al., 1996) as well as to protein surface sites, where their binding modes can provide an information base for rational drug design (Allen et al., 1996; Mattos and Ringe, 1996). Intermolecular NOEs with protein protons provide a method for the straightforward identification of the binding sites of small organic ligand molecules in aqueous solution, but the number of detectable surface binding sites tends to be small (Liepinsh and Otting, 1994, 1997; Otting et al., 1997; Ponstingl and Otting, 1997; Dalvit et al., 1999). In the present study, the deep lipid-binding pocket in the interior of non-specific lipid transfer protein (ns-LTP) from wheat was explored, using intermolecular NOEs with a variety of small organic molecules.

Plant ns-LTPs have the ability to transfer lipids between artificial membranes in vitro, but their biological role in vivo is not well established. Different functions have been proposed, including a role in cutin formation by transport of cutin monomers (Sterk et al., 1991) and a role as antimicrobial agent in plant de-

*Deceased 10 June 1998.
**To whom correspondence should be addressed.
E-mail: gottfried.otting@mbb.ki.se

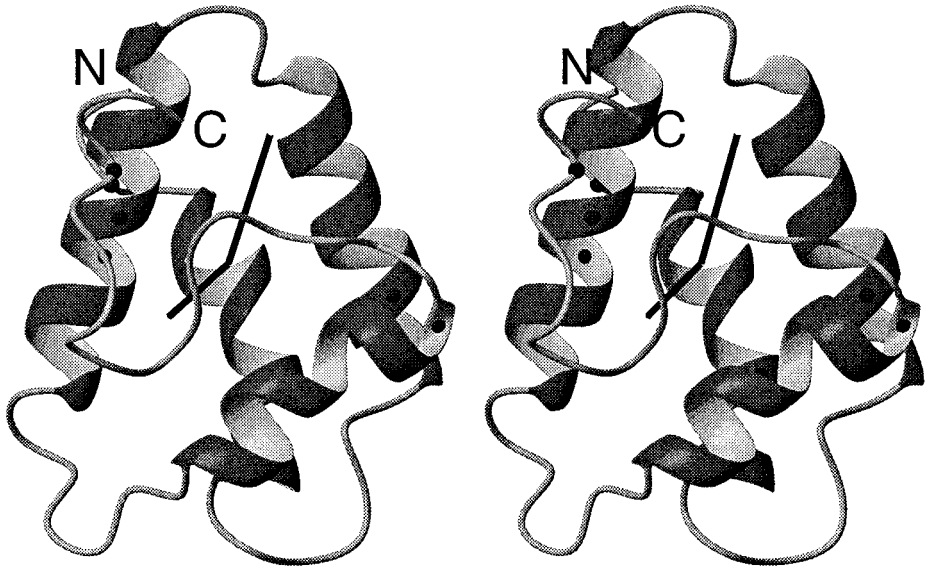

Figure 1. Stereo ribbon display of wheat ns-LTP. N- and C-termini are labelled, the positions of the C^{α} atoms of cystine residues are identified by spheres, and the lipid-binding site is outlined by a bar with a kink. This figure and Figure 6 were drawn with MOLMOL (Koradi et al., 1996).

fense against pathogens (Garcia Olmedo et al., 1995). The lipid-binding site in ns-LTP can be described as a shallow basket formed by helices 1 and 2 at the bottom, helices 3 and 4 at the sides, and with the C-terminal loop of 15 residues as a lid (Figure 1). The structure is stabilized by four disulfide bridges, linking the N- and C-termini to helix 3, and helices 1 and 4 to helix 2. The structure of wheat ns-LTP has been determined both with and without bound lipid (Gincel et al., 1994; Sodano et al., 1997; Charvolin et al., 1999). In spite of its irregular secondary structure, the C-terminal loop after helix 4 assumes a defined conformation, maintaining about 380 $Å^3$ of hydrophobic cavity space in the absence of lipid (Gomar et al., 1997). Upon binding of a lipid with two fatty acid side chains, this space is enlarged to about 750 $Å^3$ (Sodano et al., 1997). As the most significant amide proton frequency shifts were observed for helix 4 and the C-terminal segment, it appears that the largest conformational changes upon ligand binding occur in the C-terminal region. As in maize ns-LTP (Shin et al., 1995), the polar head group of the lipid is largely solvent exposed and located at the top end of the molecule in the orientation of Figure 1 (Sodano et al., 1997).

Compared to wheat and maize ns-LTP, the opposite orientation was observed for palmitate complexed to barley ns-LTP (Lerche and Poulsen, 1998) while a crystal structure of wheat ns-LTP with two lipid molecules bound showed both orientations in the same complex (Charvolin et al., 1999). Binding of the bulkier palmitoyl CoA ligand to barley ns-LTP resulted in an expanded structure, primarily achieved by an outward movement of helix 3 (Lerche et al., 1997). Barley ns-LTP, like rice ns-LTP, has only very little hydrophobic cavity space in the unliganded state, illustrating the readiness of structural expansion upon lipid binding (Lee et al., 1998). On the other hand, a homologous protein with little internal cavity space, *Ace*-AMP1, does not bind lipids (Tassin et al., 1998).

The ability of plant ns-LTPs to accommodate different sized ligands makes them interesting for biotechnological applications. The present study was performed to explore the use of small organic molecules as probes for the detection of the large internal hydrophobic pocket in wheat ns-LTP, its preference for molecules of different size and polarity, and its readiness to expand to capture larger organic solvent molecules.

Methods

Sample conditions and resonance assignments

All NMR experiments were performed with a ca. 10 mM aqueous solution of wheat ns-LTP. The original structure determination of wheat ns-LTP had been performed at pH 6.0 and 35 °C (Gincel et al.,

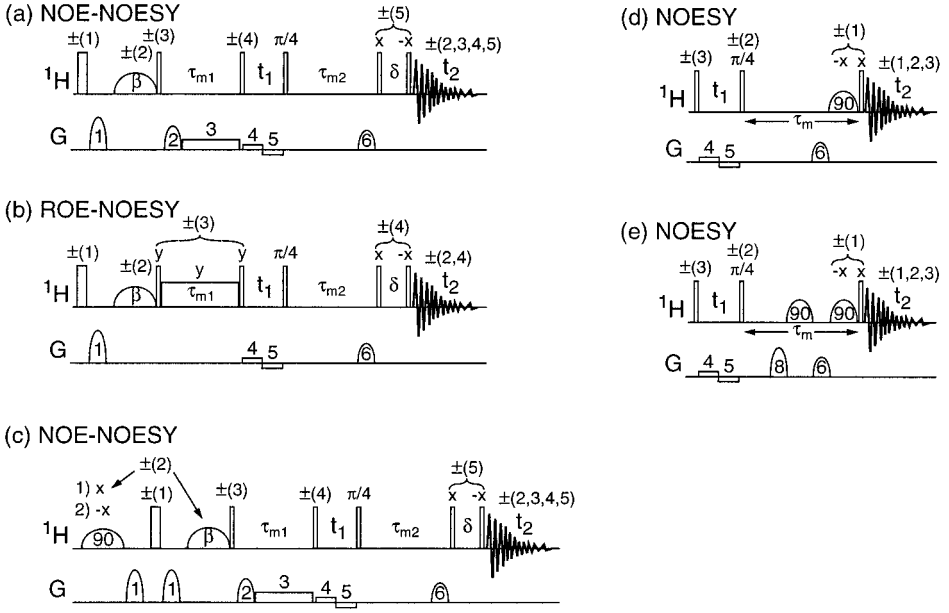

Figure 2. Pulse sequences used to measure intermolecular NOEs with water and organic cosolvents. Wide and narrow bars represent 180° and 90° pulses, respectively. Rectangular shapes of lower amplitude represent spin-lock mixing times. Round shapes indicate selective Gaussian pulses (Bauer et al., 1984). Gradient pulses were applied either as sine-shaped or rectangular pulses (round and rectangular shapes in the figure). Gradient strengths (durations) were: $G_1 = 7.5$ (1.0), $G_2 = 5$ (2.0), $G_3 = 0.5$ (τ_{m1}), $G_4 = 0.25$ ($t_1/2$), $G_5 = -0.25$ ($t_1/2$), $G_6 = 2.5$ (1.5), $G_7 = 15$ (1.0), $G_8 = 5$ (1.0) G/cm (ms), respectively. Any gradient stronger than 1 G/cm was followed by a 1 ms recovery delay. All pulses were applied with phase x unless indicated differently. Phase cycles are indicated by identifying phase-alternated pulses by ± signs. The same numbers are shown with the receiver phase, when the receiver phase is alternated together with the respective pulse phase. For example, the explicit phase cycle of the ROE-NOESY experiment in (b) is: 180° = x,−x; β = x,x,−x,−x; 1st 90°, spin-lock and 2nd 90° = 4(y),4(−y); 4th 90° = 8(x),8(−x); 5th 90° = 8(−x),8(x); receiver = 2(x,x,−x,−x),2(−x,−x,x,x). The 3rd 90° pulse is of constant phase, but phase-shifted by 45° relative to phase x. The β degree pulse was a 25 ms Gaussian pulse of low amplitude, adjusted to result in an effective 90°_x rotation of the inverted water magnetization by radiation damping. (a) NOE-NOESY. $\tau_{m1} = 60$ ms, $t_{1max} = 41$ ms, $\tau_{m2} = 150$ ms, $\delta = 120$ µs, $t_{2max} = 315$ ms. (b) ROE-NOESY. $\tau_{m1} = 30$ ms, $t_{1max} = 41$ ms, $\tau_{m2} = 150$ ms, $\delta = 120$ µs, $t_{2max} = 157$ ms. The mixing spin-lock was applied with a field strength of 3600 Hz. (c) NOE-NOESY for simultaneous observation of water–protein and benzene–protein NOEs. Two data sets were recorded, differing only in the phase of the initial, selective 90° pulse which was an 80 ms Gaussian pulse applied to the benzene resonance. The sum and difference of the two data sets result in NOE-NOESY spectra for water–protein and benzene–protein NOEs, respectively. $\tau_{m1} = 60$ ms, $t_{1max} = 41$ ms, $\tau_{m2} = 150$ ms, $\delta = 120$ µs, $t_{2max} = 157$ ms. (d) NOESY. Radiation damping during the mixing time results in a water flip-back effect. The selective 90° pulse on the water resonance was a 5 ms Gaussian pulse. $t_{1max} = 41$ ms, $\tau_m = 60$ ms, $t_{2max} = 157$ ms. (e) NOESY. The first selective 90° pulse was a 5 ms Seduce pulse element (McCoy and Mueller, 1992) on the dioxane resonance. $t_{1max} = 41$ ms, $\tau_m = 70$ ms, $t_{2max} = 157$ ms. ^{13}C-decoupling during the first selective pulse and t_2 was used to eliminate the ^{13}C satellites of the dioxane signal.

1994). Preliminary experiments showed that water–protein NOESY cross peaks were more intense at pH 4.0 and 15 °C. Subsequently, all experiments in the present study were performed at this pH and temperature. The pH was not adjusted after addition of organic solvents or gases to the solution. The resonance assignments of wheat ns-LTP were established by NOESY and TOCSY spectra and comparison with the assignments used for the structure determination. Experiments were performed on a Bruker DMX 600 NMR spectrometer.

NMR pulse sequences

Intermolecular NOEs with water and organic solvent molecules were recorded using the pulse sequences shown in Figure 2. The NOE-NOESY pulse sequence of Figure 2a was found to yield maximum sensitivity by providing a high yield of both selective water excitation and water flip-back. The excitation scheme has been described earlier (Liepinsh and Otting, 1995). Briefly, all magnetization is inverted non-selectively, radiation damping is suppressed by the following pulsed field gradient, and the water magnetization is selectively excited by the following Gaussian-shaped small flip-angle pulse which triggers radiation damping. This selective pulse was adjusted in phase and

amplitude so that the water magnetization was aligned along the ±y axis after a 25 ms pulse. Water magnetization exchanges with the protein during the mixing time τ_{m1} during which radiation damping is suppressed by a short, relatively strong gradient pulse followed by a continuous weak gradient during the remaining part of the mixing time. The rest of the pulse sequence represents a conventional NOESY experiment. Bipolar gradients (Sklenář, 1995) during t_1 result in a narrow line width of the water resonance in the F_1 frequency dimension. The mixing time τ_{m2} was chosen for maximum sensitivity of the intra-protein NOEs. Radiation damping during τ_{m2}, combined with a 45° phase shift of the first 90° pulse after t_1, results in water magnetization aligned along the positive z axis by the end of τ_{m2} (Driscoll et al., 1989). A gradient defocuses residual transverse water magnetization. The following jump-return sequence (Plateau and Guéron, 1982) reads out the protein magnetization with a minimum of signal loss by transverse relaxation, while returning the water magnetization to the z axis, which allows rapid repetition rates without much attenuation of the water magnetization in the steady state. The ROE-NOESY pulse sequence of Figure 2b was constructed according to the same principles.

By fortuitous coincidence, the ^{1}H resonance of benzene was resolved in the protein ^{1}H NMR spectrum. At the same time, it was much narrower than the protein resonances. Therefore, it could be selectively excited with good yield by an 80 ms Gaussian pulse. The NOE-NOESY pulse sequence of Figure 2c was used to record the intermolecular NOEs with water in the presence of benzene. At the same time, the experiment yielded a second data set representing an NOE-NOESY with benzene instead of water. The pulse sequence is identical to that of Figure 2a, except that it is preceded by a long selective 90° pulse applied to the benzene resonance and a gradient pulse of the same strength as the gradient pulse after the following non-selective 180° inversion pulse, resulting in refocusing of the transverse benzene magnetization. Since the benzene resonance is a singlet, there is no scalar coupling evolution during these time periods and the phase of the selective 90° pulse on benzene can be adjusted to align the benzene magnetization along the y axis before the first non-selective 90° pulse. Two data sets are recorded with different phase of the benzene-selective pulse. Summation results in the NOE-NOESY for water–protein NOEs, whereas the difference represents the NOE-NOESY with benzene–protein NOEs. While the experiment does not compromise the sensitivity of the water–protein NOEs, the NOEs with benzene are attenuated due to transverse relaxation during the selective excitation scheme.

Since the chemical shifts of wheat ns-LTP were sensitive to the solvent composition, non-selective 2D NOESY spectra were recorded to reassign the protein resonances for each new cosolvent. The experiments were recorded both with a jump-return sequence as the 'read-out' sequence before the evolution time, as in Figure 2a, or with the combination of a relatively short, water-selective 90° pulse followed by a non-selective 90° pulse of opposite phase, as in Figure 2d (Sklenář and Bax, 1987), trading clean phases in the F_2 dimension near the water resonance for uniform excitation over a large spectral range distant from the water signal. Radiation damping during the mixing time provided a water flip-back effect without affecting the cosolvent–protein NOEs. The sine-shaped excitation profile of spectra recorded with the jump-return sequence as the read-out sequence was corrected after Fourier transformation by appropriate scaling of the data. The high concentration of dioxane required additional measures to suppress the dioxane resonance before detection. This was achieved by a short, dioxane-selective 90° pulse towards the end of the mixing time, followed by a gradient pulse (Figure 2e).

Selective excitation of most of the organic cosolvents was complicated by overlap with protein resonances. In these cases, experiments for the selective observation of intermolecular NOEs were performed by NOESY experiments with a spin-echo sequence inserted before the evolution time t_1, during which the protein signals relaxed by T_2 relaxation (Liepinsh and Otting, 1997). For example, intermolecular NOEs with acetonitrile were recorded with the 1D NOE experiment described by Stott et al. (1997), using a double pulsed field-gradient spin echo (DPFGSE) with 40 ms Gaussian-shaped 180° pulses for selective excitation of the acetonitrile resonance and a non-selective 180° pulse in the middle of the NOE mixing time to prevent the recovery of protein magnetization. The total excitation sculpting delay was 300 ms, which strongly suppressed the protein magnetization. In the case of cyclohexane, only non-selective experiments were performed, because any spin-echo delay also resulted in significant reduction of the cyclohexane signal.

NOEs with cyclopropane, ethane and methane were recorded with a 5 mm sapphire tube (Cusanelli et al., 1996) using non-selective NOESY experiments.

In addition, a 1D NOE experiment was recorded with methane using an 80 ms 90° Gaussian pulse for selective excitation of the methane resonance. Since the ^{1}H resonance of ethane overlapped with the methyl resonances of LTP, one of the experiments was recorded with the scheme of Ponstingl and Otting (1997), where intra-protein NOEs and the solute signal are suppressed by a spin-echo delay before t_1 and a diffusion filter of 19 ms duration before t_2, respectively. The experiment was performed as described (Ponstingl and Otting, 1997), except that the gradient pulses during the diffusion filter were applied with 3 ms rather than 2 ms duration.

NMR spectra in the gas phase

The vapour pressure of the different organic solvents in the aqueous solutions was measured by placing a drop of the solvent mixture at the bottom of a 5 mm NMR tube and measurement of the NMR spectrum of the gas phase above the solvent. The resonances of the vapor phases were well resolved due to large chemical shift differences between the vapor and solution phases. Diffusion experiments discriminated the vapor phase signals from the resonances of solvent condensed at the glas wall of the NMR tube. Furthermore, the vapor phase signals were characterized by short T_1 relaxation times of the order of 100 ms. For quantitative signal integration, a capillary filled with TSP in D_2O was inserted to provide a reference standard. The intensity of the TSP signal in the capillary was calibrated by comparison with the signal integral of a known quantity of glycine dissolved in water.

Results and discussion

Occupancies from intermolecular NOEs

The intensities of intermolecular NOEs between proteins and solvent molecules depend on the internuclear distance, the occupancy of the solvation site and the residence time and mobility of the solvent molecules. Residence times shorter than about 0.3 ns give rise to positive water–protein NOEs at 600 MHz ^{1}H frequency (i.e. negative cross peaks in NOESY spectra), whereas residence times longer than about 1 ns result in negative NOEs, which increase in intensity with the residence time as long as the residence time is shorter than the rotational correlation time of the protein (Otting et al., 1991; Otting, 1997).

The interpretation of intermolecular NOEs in terms of occupancies requires that effects from residence times and local mobility can be excluded. For example, if a solvent molecule reorientates isotropically at its binding site on a time scale much faster than the reorientation rate of the protein, the intermolecular NOEs correspond to the NOE with a hypothetical proton at the center of the binding site (Otting et al., 1997). This case is perhaps best approximated by a rapidly rotating methane molecule bound to an internal cavity with space for exactly one methane molecule and a residence time longer than the rotational correlation time of the protein (nanoseconds). Long residence times are indicated when the absolute magnetization transfer rate in the laboratory frame, $|\sigma^{NOE}|$, is not much less than half of the corresponding rate in the rotating frame, σ^{ROE}, and $\sigma^{NOE} < 0$ (Otting, 1997). To date, positive intermolecular NOEs with proteins have been reported exclusively for highly solvent-accessible water, whereas NOEs with organic solvents are negative or too weak to be observed. Small solvent molecules, like water and methane, in internal protein cavities are characterized by residence times of at least 1 ns (Denisov and Halle, 1996; Otting et al., 1997). Much larger molecules, like benzene and cyclohexane, would be expected to have longer residence times, so that a qualitative interpretation of intermolecular NOE intensities in terms of occupancies may be justified.

Intermolecular NOEs with water

Intermolecular NOEs between protons lining a hydrophobic cavity in human interleukin-1β and water have been reported to be of comparable intensity as NOEs with water molecules at well-defined hydration sites in the protein interior, suggesting high water occupancy (Ernst et al., 1995). Although we observed many water–protein cross peaks in the NOE-NOESY spectrum of wheat ns-LTP (Figure 3a), most of these can be explained by chemical exchange with water or by exchange-relayed NOEs with exchangeable NH and OH protons from the protein (Otting, 1997), and no NOE could be unambiguously attributed to internal hydration water molecules. In particular, many of the protons lining the hydrophobic pocket in uncomplexed wheat ns-LTP are within 5 Å of the exchangeable NH and OH protons of the side chains of His35 and Tyr79, which form part of the pocket lining in the refined NMR structure (Denise Sy, unpublished results) and exchange rapidly with the water. No off-diagonal peaks could be identified in the NOE-NOESY spectrum for the isopropyl groups of Val10 and Leu51, which are centrally located in the pocket, yet remote from His35 and Tyr79. In the NOE-NOESY spec-

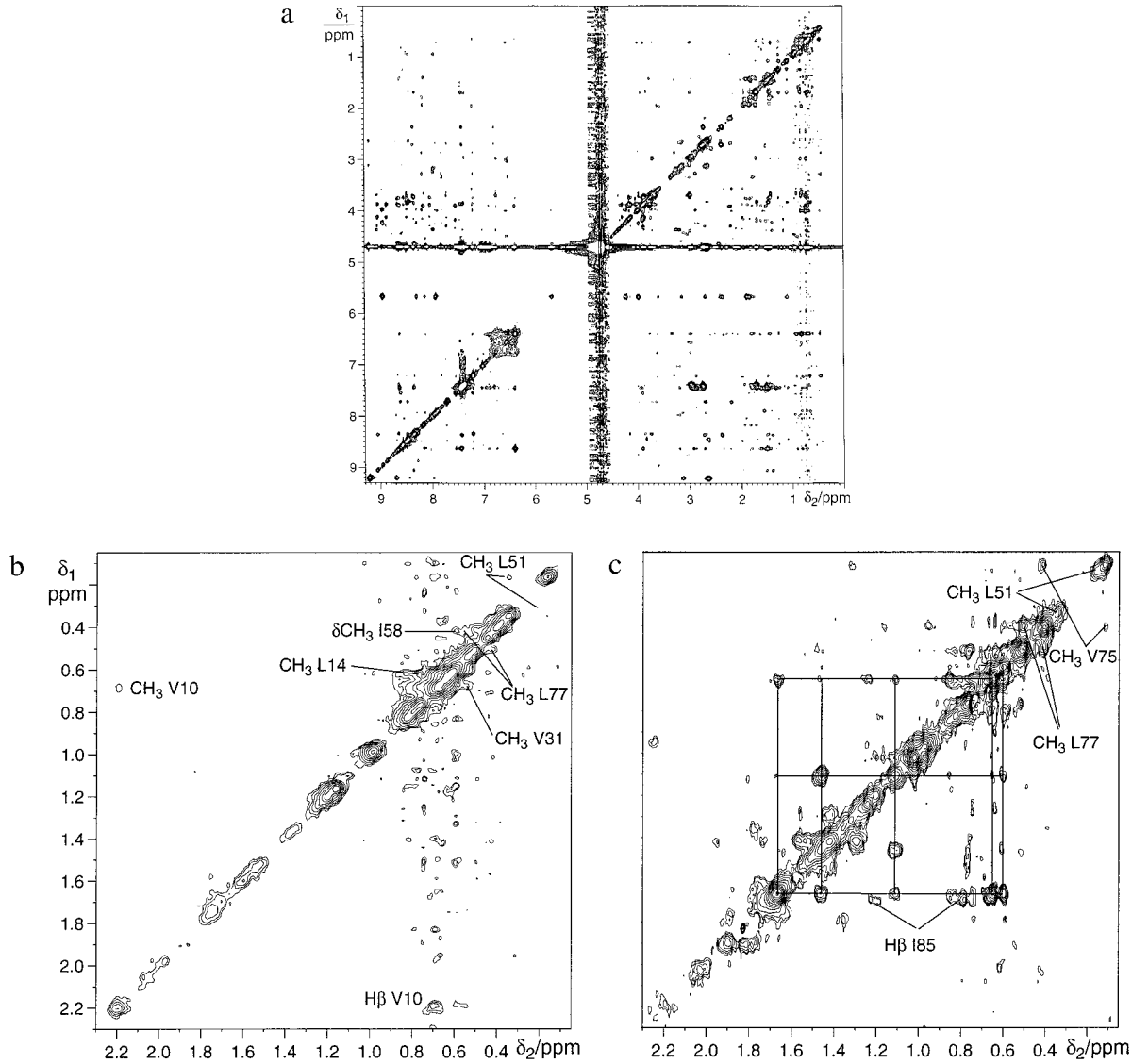

Figure 3. NOE-NOESY spectra recorded with an aqueous solution of wheat ns-LTP in the absence and presence of a saturating amount of benzene at pH 4 and 15 °C. (a) Overview of the NOE-NOESY spectrum recorded in aqueous solution with the pulse sequence of Figure 2a, using a total experimental time of 44 h. (b) High-field region of the benzene subspectrum of the NOE-NOESY experiment recorded in 16 h in the presence of benzene. The diagonal peaks arise from magnetization transfer between benzene and wheat ns-LTP. Off-diagonal peaks are identified with the assignment of the proton involved in an NOE with benzene. (c) High-field region of the water subspectrum from the same NOE-NOESY experiment as the benzene subspectrum shown in (b). The diagonal peaks arise from magnetization transfer between water and wheat ns-LTP. Off-diagonal peaks are identified with the assignment of the proton which received its magnetization from the water resonance. Vertical and horizontal lines connect peaks from Ile1 which probably represent exchange-relayed NOEs with the N-terminal amino group.

trum recorded in the presence of benzene, the methyl resonances of Leu51 were shifted to high field, allowing their identification on the diagonal (Figure 3c). Although these diagonal peaks were of comparable intensity in the water (Figure 3c) and benzene (Figure 3b) subspectra, the NOEs were relatively weak, as the excitation scheme of this experiment selectively attenuates the benzene magnetization (see above). In comparison, the exchange-relayed NOEs with the N-terminus of wheat ns-LTP or the isopropyl group of Leu77, which is close to His35 and Tyr79, were much stronger than the NOEs between water and Leu51 (Figure 3c). A corresponding ROE-NOESY spectrum recorded with the pulse sequence of Figure 2b did not

show new water–protein cross peaks or off-diagonal peaks of higher intensity than the NOE-NOESY spectrum, indicating that the water-LTP NOEs are not quenched by water exchange in the 0.3–1 ns time range, where σ^{NOE} would be much smaller than σ^{ROE} (Otting, 1997).

One may assume that any water molecules in the hydrophobic pocket would undergo considerable motions, resulting in weaker NOEs similar to the situation observed with methane (see below). Notably, however, the intermolecular water–protein NOEs were weak even when the solvent-accessible space was restricted by the presence of benzene.

Intermolecular NOEs with benzene

In a saturated aqueous solution of benzene, each wheat ns-LTP molecule binds about three molecules of benzene, as judged from the relative signal integrals in the 1D ^{1}H NMR spectrum after subtraction of the benzene concentration in pure water (ca. 14 mM at 15 °C). Since the ^{1}H NMR resonance of benzene was resolved, intermolecular NOEs with wheat ns-LTP could be observed with high sensitivity in simple 1D NOE experiments (Figure 4). The corresponding 1D ROE spectrum shows that most NOEs are direct, whereas spin-diffusion may have generated the cross peaks with the amide protons in the 1D NOE spectrum. Strong NOEs were observed with the methyl groups of the protein. With few exceptions, all protons for which intermolecular NOEs with benzene were unambiguously identified in the 1D NOE and 2D NOE-NOESY spectra (Table 1 of Supplementary material) are located in the vicinity of the hydrophobic pocket in wheat ns-LTP (Figure 6a). The exceptions are Lys52, Ala55 and Ile58, which are near or at the outer protein surface. Apparently, benzene can enter the hydrophobic pocket in wheat ns-LTP, but also finds binding sites on the protein surface.

A positive NOESY cross peak was observed between benzene and water, as would be expected for an NOE between molecules with residence times longer than a few nanoseconds. The cross peak could, however, also be interpreted as an exchange-relayed NOE with Tyr79 OH, which is broadened beyond detection in the presence of benzene (see below).

Selective line-broadening by a few Hz was observed for the amide protons of residues 6, 7, 10, 38, 50, 51, 55 and 81. The same and more amide proton resonances broadened more strongly in the presence of cyclohexane. This suggests that the line-broadening results from an exchange between different protein conformations rather than different ligand orientations.

An attempt was made to define the binding sites of benzene from the chemical shift changes observed upon complexation. Some of the chemical shift changes observed were larger than 0.5 ppm, but their magnitude did not correlate with the observation of intermolecular NOEs. The overlapping ring current effects from several benzene molecules, possibly combined with small structural changes of the protein, made any interpretation difficult.

Complex with cyclohexane

The relative signal intensities in the 1D ^{1}H NMR spectrum indicated that three molecules of cyclohexane bound to each molecule of wheat ns-LTP in the presence of a liquid cyclohexane phase on top of the aqueous protein solution. The chemical shift changes were generally smaller than with benzene, with maximum values of about 0.25 ppm for the assigned amide protons. However, several of the protein resonances, in particular amide proton resonances, were affected by exchange-broadening, preventing their assignment. Figure 6b shows that the exchange-broadened amide proton resonances were mostly located in helix 3 (residues 48–55) and in the C-terminal segment (residues 66–85). Possibly, helix 3 responds to the bulky cyclohexane molecules by moving outwards, in analogy to the shift of helix 3 observed in barley ns-LTP upon binding of palmitoyl CoA (Lerche et al., 1997).

Only few intermolecular NOEs between cyclohexane and wheat ns-LTP could be assigned, because of spectral overlap in the NOESY spectrum and incomplete resonance assignments. Yet, the few unambiguous assignments which were made demonstrate that cyclohexane enters the hydrophobic pocket (Figure 6b). In addition, the NOE with Ile58 suggests a binding site on the protein surface. A small positive NOESY cross peak was observed between water and cyclohexane, which could be interpreted as a direct NOE or an exchange-relayed NOE with Tyr79 OH, as in the case with benzene.

Measurements with dioxane

In order to test the hydrophobic pocket in wheat ns-LTP for its preference for hydrophobic molecules, a NOESY spectrum was recorded in the presence of 5% v/v dioxane, but no intermolecular NOEs could be detected (data not shown). At the sensitivity of the experiment, intermolecular NOEs at least 20 times

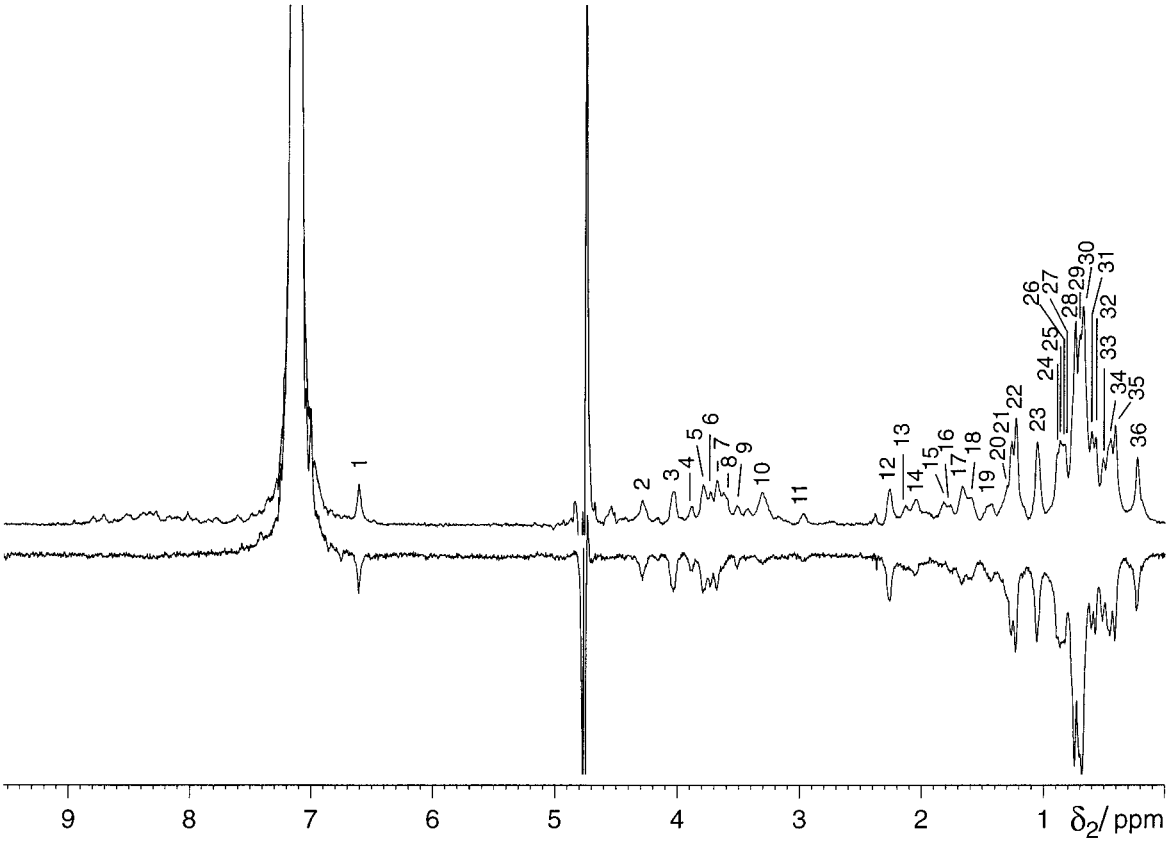

Figure 4. Intermolecular NOEs between benzene and wheat ns-LTP at 15 °C. The 1D NOE (upper panel) and ROE (lower panel) experiments were recorded in 1.5 h each, using 60 ms mixing time. See Supplementary material for the pulse sequences used and the resonance assignments of the cross peaks.

weaker than those observed between cyclohexane and wheat ns-LTP would have been observable.

Under the conditions used for the NOESY spectrum, there was also no evidence for binding from chemical shift changes. Small chemical shift changes in the 1D ^{1}H NMR spectrum of wheat ns-LTP were observed first at 10% v/v dioxane concentrations and higher, which may reflect indirect effects from the altered solvent conditions. Since cyclohexane and dioxane are similarly shaped molecules, we conclude that dioxane is not easily accommodated in the hydrophobic pocket because of its polarity.

Intermolecular NOEs with acetonitrile

Since wheat ns-LTP seems to expand its hydrophobic pocket to accommodate cyclohexane, the entry of dioxane must be hindered by its size as well as its polarity. In order to test whether a smaller sized polar molecule would enter the hydrophobic pocket, NOESY data were recorded in the presence of 5% v/v acetonitrile. Figure 5a shows that intermolecular NOEs could be observed, but only the NOEs with Leu77 and Tyr79 could be assigned unambiguously. Yet, these NOEs and the ambiguous assignments with the methyl groups indicate that acetonitrile enters the hydrophobic cavity (Figure 6c). The interaction seemed to be relatively weak, as the NOE intensities with the methyl groups of wheat ns-LTP were about eight-fold weaker than those observed with cyclohexane, and the maximum chemical shift change observed for a backbone amide proton was only 0.15 ppm.

Intermolecular NOEs with cyclopropane, ethane and methane

Cyclopropane, ethane and methane are small organic gas molecules which are suitable probes for hydrophobic cavities (Liepinsh et al., 1997; Otting et al., 1997). The ^{1}H NMR signals of cyclopropane and methane in water were outside the chemical shift range of

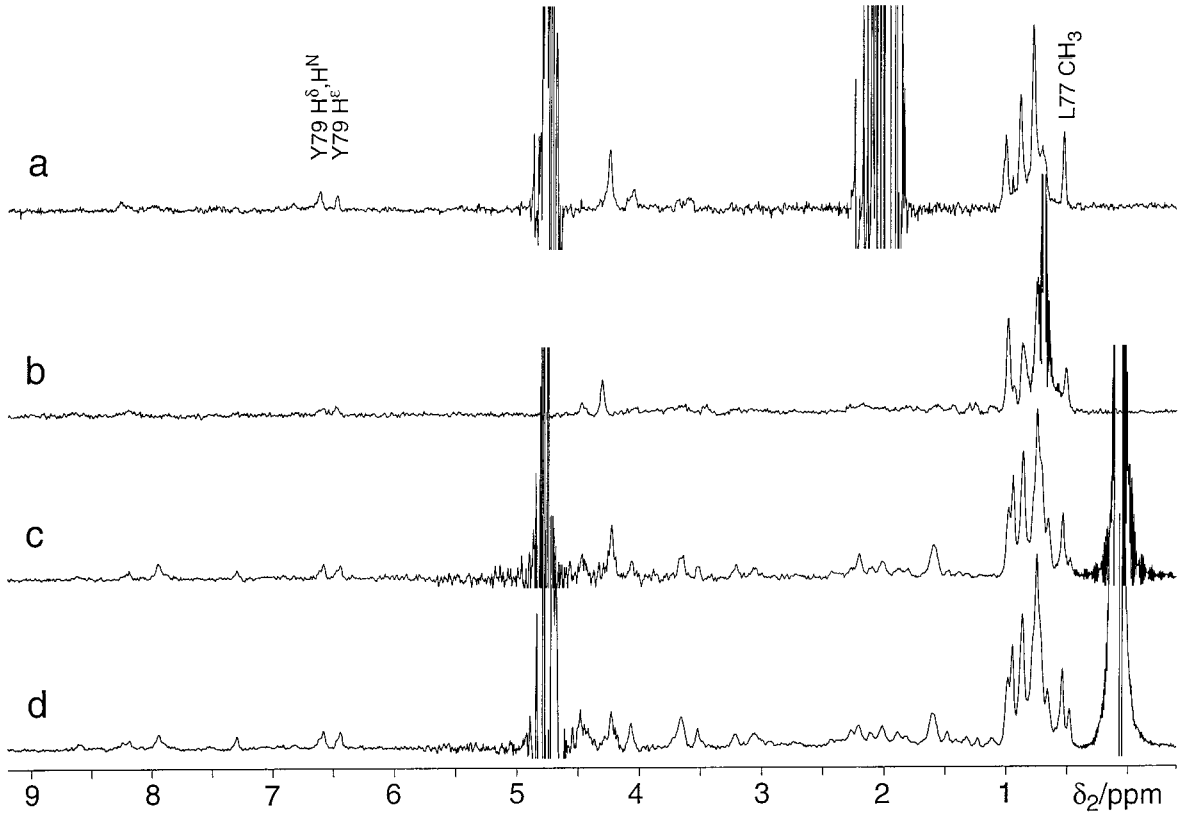

Figure 5. Intermolecular NOEs between small organic molecules and wheat ns-LTP at 15 °C and pH 4.0 (measured before addition of the cosolvents). (a) NOEs with acetonitrile. The spectrum was recorded as a 1D NOE experiment in 12.5 h with a mixing time of 100 ms, using excitation sculpting for selective excitation of the acetonitrile resonance during a 300 ms delay. (b) NOEs with ethane. The spectrum was recorded with the experimental scheme of Ponstingl and Otting (1997), using $t_{1max} = 39$ ms, $\tau_m = 300$ ms, $t_{2max} = 157$ ms, 40 bar ethane pressure, and a total experimental time of 36 h. (c) NOEs with methane. Spectrum recorded with the pulse sequence of Figure 2d, except that a jump-return sequence was used for water suppression. $t_{1max} = 61$ ms, $\tau_m = 300$ ms, $t_{2max} = 157$ ms, 140 bar methane pressure, total experimental time 20 h. (d) NOEs with cyclopropane recorded in the presence of liquid cyclopropane on top of the aqueous protein solution. Same spectral parameters as in (c), except that $t_{1max} = 69$ ms. Spectra (b)–(d) are cross sections through the diagonal peaks of the gas molecules in 2D NOESY spectra.

wheat ns-LTP, so that conventional 2D NOESY spectra could be used for the detection and assignment of the intermolecular NOEs. In contrast, the ethane signal overlapped with the methyl resonances of the protein, requiring the use of relaxation and diffusion filters (Ponstingl and Otting, 1997) to resolve the intermolecular NOEs.

Cyclopropane was used at about 5 bar pressure, resulting in a liquid cyclopropane phase on top of the aqueous protein solution. Comparison of the intermolecular NOEs with methane or ethane (Figure 5c and b) with those observed with acetonitrile (Figure 5a) shows close similarity in the spectral region of the methyl protons. As with acetonitrile, NOEs with Leu77 and the side chain protons of Tyr79 were unambiguously assigned. Methane and cyclopropane displayed the same intermolecular NOEs in a NOESY spectrum recorded in the simultaneous presence of cyclopropane and methane at 70 bar (data not shown). This shows that all these gases fill the same space of the hydrophobic pocket and indicates that the small chemical shift differences observed between the spectra with methane (Figure 5c) and cyclopropane (Figure 5d) are caused by the anisotropy effect of cyclopropane rather than by structural changes of the protein. The inertness of the protein structure is also reflected by the small chemical shift changes (< 0.05 ppm) observed between ns-LTP with and without methane.

The intermolecular NOEs with the protein were of the same sign as the intra-protein NOEs. Gas diffusion in the hydrophobic pocket space thus does not

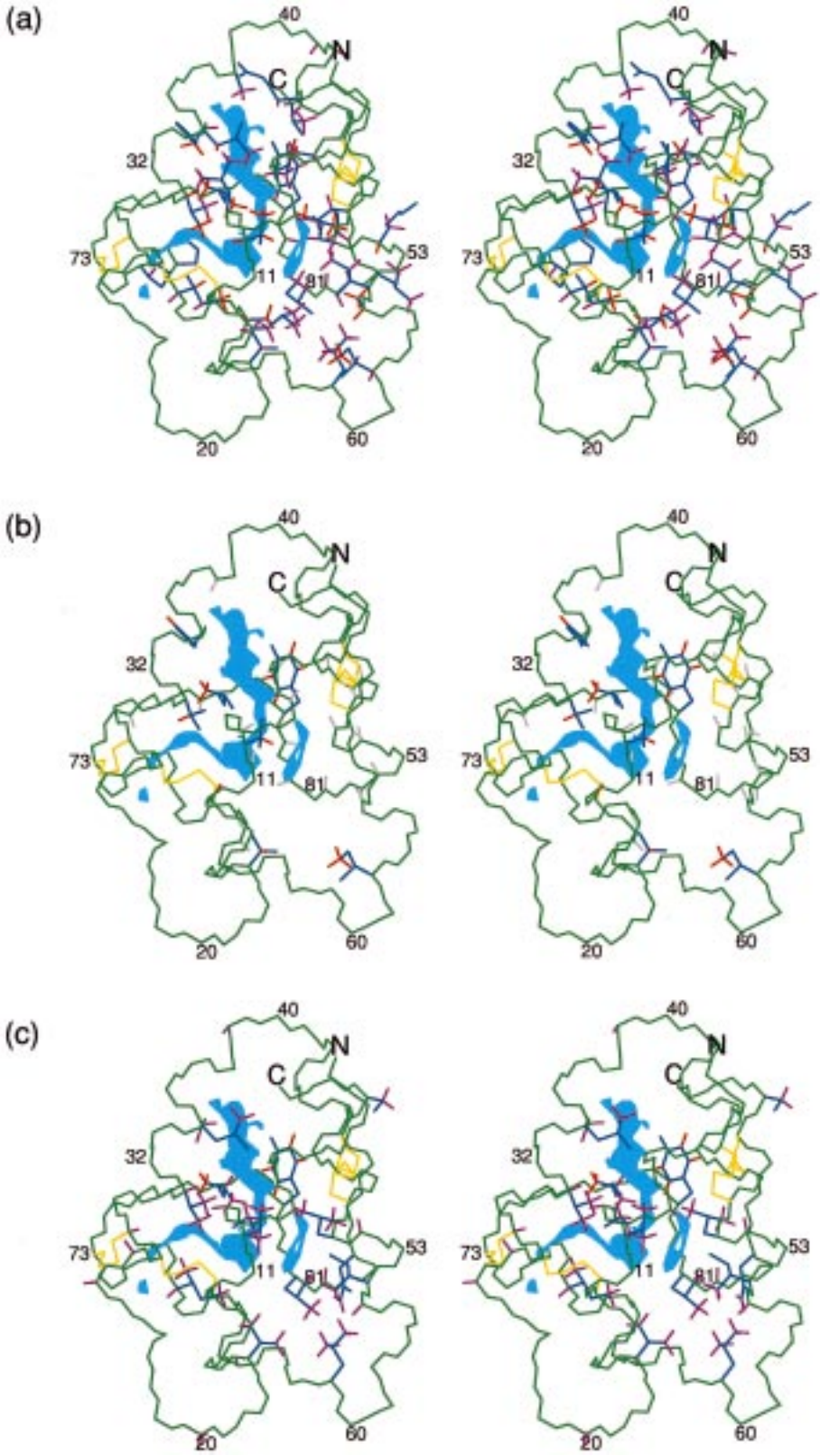
(a)
(b)
(c)
N
C
40
32
73
53
11
81
20
60

Figure 6. Stereo representations of wheat ns-LTP showing the protons involved in intermolecular NOEs with organic solvent molecules. The molecule is shown in an orientation rotated by 180° around a vertical axis compared to that of Figure 1. Green: backbone; yellow: disulfide bridges; dark blue: bonds connecting the heavy atoms of those amino acid side chains which carry protons for which intermolecular NOEs were ambiguously or unambiguously assigned. Only those side chains are displayed for which intermolecular NOEs were assigned. The locations of selected residues are identified by their sequence numbers. The hydrophobic pocket in the interior of the structure is visualized by a light blue colour on coordinate points, where a sphere of 1.4 Å radius could be placed without van der Waals violations with the protein structure. The volume of the pocket varies between different NMR conformers and is about 440 $Å^3$ in the structure shown. (a) Intermolecular NOEs with benzene. Orange: covalent bonds with protons for which intermolecular NOEs were unambiguously assigned; magenta: covalent bonds with protons for which intermolecular NOEs may be present, but unambiguous assignments could not be made due to spectral overlap. (b) Intermolecular NOEs with cyclohexane. Same colour coding as in (a), except that ambiguous NOE assignments are not displayed. In addition, NH bonds of amide protons are shown in grey when the corresponding ^{1}H resonances were broadened or could not be assigned because of excessive line-broadening. The NOE with the side chain of His35 does not indicate a surface binding site, as the χ_2 angle of this side chain is undetermined in the NMR structure of wheat ns-LTP. (c) Intermolecular NOEs with acetonitrile. Same color code as in (a).

shorten the residence times to subnanosecond values, where the sign of the intermolecular NOE would be inverted. The intermolecular water–methane, water–ethane and water–cyclopropane NOEs were positive, probably reflecting interactions in the bulk solvent.

Occupancies in the hydrophobic pocket

Integration of the intensities of the intermolecular NOEs between the organic molecules and the methyl groups of wheat ns-LTP (spectral region about 0.6 to 1.1 ppm) yielded the following relative NOE intensities: benzene (saturated in water) > cyclohexane (saturated in water) > acetonitrile (5% v/v in water) > ethane (40 bar) > methane (140 bar) > cyclopropane (saturated in water), with approximate intensity ratios of 10:5.6:0.7:0.3:0.2:0.1. NOEs with dioxane were at least 20 times weaker than with cyclohexane, as none could be detected. For comparison, all NOE intensities were normalized by the well-resolved intraresidual NOE between the H^{β} protons of Pro12. Since the 2D NOESY spectra in the presence of methane and cyclopropane had been recorded with 300 ms rather than 60 ms mixing time, the intensities of these NOEs were divided by 20 for comparison with the NOEs with the organic solvents to account for the fivefold longer mixing time and the fourfold reduction of the intensity of the reference cross peak of Pro12 observed in NOESY spectra of the free protein recorded at these two mixing times. Different relaxation delays had been used to record the NOESY spectra (1.3 s for cyclohexane and dioxane, 1.5 s for acetonitrile, 2.0 s for methane and cyclopropane, 2.3 s for benzene, 4.0 s for ethane). Therefore, the intensity ratios listed above are corrected for incomplete recovery of equilibrium magnetization during the relaxation delays, using the experimentally determined T_1 relaxation times of the different cosolvents (0.35 s for dioxane, 0.4 s for acetonitrile, 1.1 s for cyclohexane, 2.3 s for benzene, 2.3–3.2 s for methane between 20 and 190 bar, 3.0 s for ethane) and assuming recovery from completely saturated magnetization. There is a clear trend for larger solvent molecules to yield larger NOEs than small gas molecules.

As benzene and cyclohexane do not dissolve in water very well, the number of benzene and cyclohexane molecules bound to wheat ns-LTP could be estimated simply from their signal intensities measured in the 1D ^{1}H NMR spectrum. The number of bound benzene and cyclohexane molecules determined in this way corresponded to very high occupancies in the hydrophobic pocket. A similar estimate was not possible for the other organic molecules used, because of their solubility in water. In addition, the small chemical shift changes induced by the gas molecules could not be used to derive binding constants. Consequently, methane occupancies were estimated by monitoring the intensity of the intermolecular NOEs as a function of methane concentration (Figure 7). In a simple analysis, where complex formation is represented by a single binding constant between methane and protein molecules and non-cooperative binding is assumed, the dependence of the NOE intensity I on the binding constant K and the methane concentration $[m]$ can be described by

$$I = I_c K[m]/(1 + K[m]), \quad (1)$$

where I_c is the NOE intensity at full occupancy (Liepinsh and Otting, 1994). Using this formula, the data of Figure 7 indicate about 25% occupancy at the maximum methane pressure used (190 bar). As even fourfold more intense methane–LTP NOEs would be about 10-fold weaker than the experimentally observed benzene–LTP NOEs, the methane–LTP NOEs are clearly reduced by local mobility of the methane molecules in the hydrophobic pocket.

While the present data do not provide much information about water occupancy in the hydrophobic pocket, water access to the hydroxyl proton of Tyr79

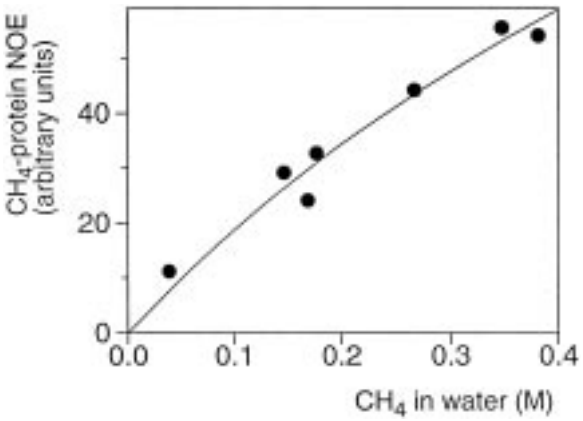

Figure 7. Intensities of the intermolecular NOEs observed between methane and wheat ns-LTP as a function of methane concentration at 15 °C, pH 4.0 (measured before addition of methane). The NOE intensities were measured in 2D NOESY spectra recorded as in Figure 5c. A repetition delay of 2 s was used between scans and the NOE intensities were corrected for the pressure-dependent T_1 relaxation rates of methane, which were independently determined by inversion-recovery experiments.

is evidenced by chemical exchange with water. This proton is located near the entry of the pocket and observable in the ^{1}H NMR spectrum at 9.2 ppm. In the uncomplexed protein and in the presence of 5% v/v acetonitrile and dioxane, this resonance was broadened to 100 Hz at half height. Cyclohexane, benzene and cyclopropane broadened the resonance beyond detection. In contrast, 140 bar methane narrowed the resonance to 38 Hz. Interestingly, the hydroxyl protons of the surface residues Tyr16 and Ser24 yielded observable resonances under all conditions with line widths of only 15 to 20 Hz.

Gas phase NMR

In a system with a protein in aqueous solution and a vapor phase, the binding of a small ligand molecule to a hydrophobic cavity in the protein can be described as an equilibrium beween the cavity and the vapor phase. Therefore, molecules with high concentration in the vapor phase would also be expected to be present in a hydrophobic protein cavity with high occupancy. Consequently, we measured the vapor phase concentrations of cyclohexane, benzene, acetonitrile (5% v/v in water), dioxane (5% v/v in water) and water at 15° by NMR spectroscopy.

The ^{1}H NMR resonances of the different solvents in the vapor/solution phase were observed at the following chemical shifts: 4.40/1.87 ppm (cyclohexane), 10.12/7.16 ppm (benzene), 4.50/2.16 ppm (acetonitrile), 4.40/3.82 ppm (dioxane), and 3.55/4.88 ppm (water). The vapor phase concentrations determined were: 0.6 mM (dioxane vapor above a solution of 5% v/v dioxane in water), 0.7 mM (water), 1 mM (acetonitrile vapor above a solution of 5% v/v acetonitrile in water), 2.5 mM (benzene) and 3 mM (cyclohexane). These data show that dioxane is five times less likely than cyclohexane to enter a hydrophobic pocket. The observation that the intermolecular NOEs with cyclohexane were more than 20-fold more intense than with dioxane may reflect unfavourable interactions of dioxane with the electrostatic fields in the hydrophobic pocket of wheat ns-LTP.

It has been argued earlier that water molecules would hardly populate small nonpolar cavities which could accommodate only single water molecules, since the concentration of water in liquid cyclohexane is comparable to that of water in the vapor phase and the energy required to form a cavity in a hydrophobic environment is small (Wolfenden and Radzicka, 1994). Furthermore, molecules larger than water were shown to prefer the hydrocarbon phase over the vapor phase, whereas molecules smaller than water prefer the vapor phase. From the vapor concentration data, water would be expected to populate the hydrophobic space in wheat ns-LTP only with incomplete occupancies. Since water is a small molecule, occupancies for single water molecules should be less than those of dioxane. Methane molecules, which are of comparable size as water molecules, are present in the vapor phase at about 8 M concentration at 190 bar, yet fill the hydrophobic pocket only incompletely. Notably, however, the presence of water in the hydrophobic environment could be favoured by hydrogen bonds between different water molecules or electric fields in the protein cavity. Electric fields might also explain the relatively strong NOEs observed between acetonitrile and wheat ns-LTP.

Conclusions

The present study shows that intermolecular NOEs between organic molecules and wheat ns-LTP are readily observed with protons lining the hydrophobic pocket of the protein. Although the hydrophobic pocket in wheat ns-LTP is about seven times larger than the volume occupied by a methane molecule in liquid methane, translational diffusion of methane in the hydrophobic pocket does not affect the sign of the intermolecular NOEs, indicating long residence times (> 1 ns). With a ^{13}C labelled sample, where

all intermolecular NOEs with methyl groups could be resolved, the NOEs would be an excellent indicator of accessible hydrophobic cavity space. Larger molecules, like benzene and cyclohexane, bind more tightly, as reflected by higher occupancies, but are more likely to cause structural changes in the protein. None of the ligands investigated bound with sufficient affinity to yield separate resonances for bound and free ligands. Since wheat ns-LTP can bind three molecules of cyclohexane, larger complexes, such as organo-metallic complexes with catalytic activity, could probably also be accommodated.

The tendency of molecules to enter the vapor phase has predictive value for their affinity to nonpolar cavities (Wolfenden and Radzicka, 1994). Gas phase NMR was found to be a simple tool for measuring concentrations in the vapor phase. The vapor pressure of water determined in this way coincided within a few percent with tabulated data.

Supplementary material

Supplementary material is available from the corresponding author. It contains 1D NOE and ROE pulse sequences used, a spectrum showing intermolecular NOEs with cyclohexane, a comparison of NOEs with methane recorded with 60 and 300 ms mixing time and a table with the resonance assignments of Figure 4.

Acknowledgements

We thank Denise Sy for the coordinates of the refined NMR structure of wheat ns-LTP. Financial support from the Swedish Natural Science Reseach Council (project 10161) is gratefully acknowledged.

References

Allen, K.N., Bellamacina, C.R., Ding, X., Jeffery, C.J., Mattos, C., Petsko, G.A. and Ringe, D. (1996) *J. Phys. Chem.*, **100**, 2605–2611.

Bauer, C., Freeman, R., Frenkiel, T., Keeler, J. and Shaka, A.J. (1984) *J. Magn. Reson.*, **58**, 442–457.

Charvolin, D., Douliez, J.-P., Marion, D., Cohen-Addad, C. and Pebay-Peyroula, E. (1999) *Eur. J. Biochem.*, **264**, 562–568.

Cusanelli, A., Frey, U., Richens, D.T. and Merbach, A.E. (1996) *J. Am. Chem. Soc.*, **118**, 5265–5271.

Dalvit, C., Floersheim, P., Zurini, M. and Widmer, A. (1999) *J. Biomol. NMR*, **14**, 23–32.

Denisov, V.P. and Halle, B. (1996) *Faraday Discuss.*, **103**, 227–244.

Driscoll, P.C., Clore, G.M., Beress, L. and Gronenborn, A.M. (1989) *Biochemistry*, **28**, 2178–2187.

Ernst, J.A., Clubb, R.T., Zhou, H.-X., Gronenborn, A.M. and Clore, G.M. (1995) *Science*, **267**, 1813–1817.

Feher, V.A., Baldwin, E.P. and Dahlquist, F.W. (1996) *Nat. Struct. Biol.*, **3**, 516–521.

Garcia Olmedo, F., Molina, A., Segura, A. and Moreno, M. (1995) *Trends Microbiol.*, **3**, 72–74.

Gincel, E., Simorre, J.P., Caille, A., Marion, D., Ptak, M. and Vovelle, F. (1994) *Eur. J. Biochem.*, **226**, 413–442.

Gomar, J., Sodano, P., Ptak, M. and Vovelle, F. (1997) *Folding Des.*, **2**, 183–192.

Koradi, R., Billeter, M. and Wüthrich, K. (1996) *J. Mol. Graph. Model.*, **14**, 51–55.

Lee, J.Y., Min, K., Cha, H., Shin, D.H., Hwang, K.Y. and Suh, S.W. (1998) *J. Mol. Biol.*, **276**, 437–448.

Lerche, M.H., Kragelund, B.B., Bech, L.M. and Poulsen, F.M. (1997) *Structure*, **5**, 291–306.

Lerche, M.H. and Poulsen, F.M. (1998) *Protein Sci.*, **7**, 2490–2498.

Liepinsh, E. and Otting, G. (1994) *J. Am. Chem. Soc.*, **116**, 9670–9674.

Liepinsh, E. and Otting, G. (1995) *J. Biomol. NMR*, **5**, 420–426.

Liepinsh, E. and Otting, G. (1997) *Nat. Biotech.*, **15**, 264–268.

Liepinsh, E., Andersson, M., Ruysschaert, J. and Otting, G. (1997) *Nat. Struct. Biol.*, **4**, 793–795.

Mattos, C. and Ringe, D. (1996) *Nat. Biotech.*, **14**, 595–599.

McCoy, M.A. and Mueller, L. (1992) *J. Am. Chem. Soc.*, **114**, 2108–2112.

Morton, A., Baase, W.A. and Matthews, B.W. (1995) *Biochemistry*, **34**, 8564–8575.

Otting, G. (1997) *Prog. NMR Spectrosc.*, **31**, 259–285.

Otting, G., Liepinsh, E. and Wüthrich, K. (1991) *Science*, **254**, 974–980.

Otting, G., Liepinsh, E., Halle, B. and Frey, U. (1997) *Nat. Struct. Biol.*, **4**, 396–404.

Plateau, P. and Guéron, M. (1982) *J. Am. Chem. Soc.*, **104**, 7310–7311.

Ponstingl, H. and Otting, G. (1997) *J. Biomol. NMR*, **9**, 441–444.

Shin, D.H., Lee, J.Y., Hwang, K.Y., Kim, K.K. and Suh, S.W. (1995) *Structure*, **3**, 189–199.

Sklenář, V. and Bax, A. (1987) *J. Magn. Reson.*, **75**, 378–383.

Sklenář, V. (1995) *J. Magn. Reson.*, **A114**, 132–135.

Sodano, P., Caille, A., Sy, D., de Person, G., Marion, D. and Ptak, M. (1997) *FEBS Lett.*, **416**, 130–134.

Sterk, P., Booij, H., Schellekens, G.A., van Kammen, A. and de Vries, S.C. (1991) *Plant Cell*, **3**, 907–921.

Stott, K., Keeler, J., Van, Q.N. and Shaka, A.J. (1997) *J. Magn. Reson.*, **125**, 302–324.

Tassin, S., Broekaert, W.F., Marion, D., Acland, D.P., Ptak, M., Vovelle, F. and Sodano, P. (1998) *Biochemistry*, **37**, 3623–3637.

Wolfenden, R. and Radzicka, A. (1994) *Science*, **265**, 936–937.